IEEE Access
Multidisciplinary ⋮ Rapid Review ⋮ Open Access Journal

Received January 5, 2022, accepted January 23, 2022, date of publication January 27, 2022, date of current version February 4, 2022.

Digital Object Identifier 10.1109/ACCESS.2022.3147019

State of the Art Sub-Terahertz Switching Solutions

JAKUB SOBOLEWSKI, (Graduate Student Member, IEEE), AND YEVHEN YASHCHYSHYN, (Senior Member, IEEE)
Institute of Radioelectronics and Multimedia Technology, Warsaw University of Technology, 00-665 Warsaw, Poland

Corresponding author: Jakub Sobolewski (j.sobolewski@ire.pw.edu.pl)

This work is part of a project IMAGE that has received funding from the European Union's Horizon2020 research and innovation programme under the Marie Skłodowska-Curie grant agreement No 778156.

ABSTRACT In this paper the state of the art in RF switches for mm-wave frequency range is summarized and evaluated. Several leading technologies is presented from typical semiconductor devices based on transistors and diodes on Si, SiGe or III-V semiconductor substrates to more unconventional solutions such as microelectromechanical or phase-change material switches. The most important parameters and characteristics for those technologies are gathered and compiled for comparison. Besides different technologies, also various switch topologies of mm-wave switches are presented, assessed and compared. Furthermore, new emerging technological solutions approaching mm-wave range involving two-dimensional materials are also presented. Their evaluation is focused on proposed designs and current results for experimentally evaluated prototypes. Although the performance of these devices are currently not competitive with more traditional approaches, some reported results near the mm-wave range makes them a promising solution for future mm-wave switches and an interesting topic for further research and development.

INDEX TERMS 2D materials, CMOS, graphene, HBT, HEMT, MEMS, millimeter wave circuits, phase-change materials, PIN diode, RF switch.

I. INTRODUCTION

Efficient millimeter wave switches are important components for development of new communication, sensing, imaging, testing and instrumentation systems [1]–[3]. Applications of such switches include switched - beam reconfigurable antennas, polarization switching, multiband receivers, transceivers, time division duplexing systems, radiometers, test circuits with multiple signal paths. Moreover, integration of the switches allows building these systems as system-on-chip millimeter wave monolithic integrated circuits (MMIC) or system-in-package solutions for greater miniaturization and increased efficiency. However, to allow on-chip integration, the switch technology has to be compatible with other parts of the integrated system such as amplifiers, digital signal processing circuits and in some cases also antennas.

There are a number of technologies available for millimeter wave switches. Most of them employs semiconductor devices produced with typical manufacturing technologies using silicon or III - V semiconductors. Among them we can distinguish transistor-based and diode-based solutions. Both bipolar (mostly heterojunction bipolar transistors - HBT) and field-effect transistors (using CMOS or high electron mobility transistor - HEMT technologies) are used in mm-wave applications. Besides them, there are less conventional technologies available such as micro electro mechanical systems (MEMS) and phase changing materials (PCM). An emerging new technology that can potentially bring significant improvements in performance of the future switching components is application of two-dimensional (2D) materials. As different technologies and types of switches excel in different parameters, it is beneficial to gather together and compare these devices in order to select the most suitable solution for particular application.

In this paper, the extensive review of state-of-the-art in mm-wave (30 to 300 GHz frequency range) switching devices is presented comparing different technologies as well as switch construction topologies. Besides the devices of highest performance, also some new technologies currently bringing considerable research interest are highlighted. These new devices at their current state of development show some

The associate editor coordinating the review of this manuscript and approving it for publication was Teerachot Siriburanon.

performance deficiencies, mostly in terms of operating frequency range, switching speed or power consumption. On the other hand, they offer low insertion loss and high isolation exceeding capabilities of state-of the art devices in more common and mature technologies.

II. TRANSISTOR - BASED SWITCHES

A. CMOS

The simplest and lowest cost semiconductor technology is a silicon complementary metal oxide semiconductor (CMOS) process. It is a well-established technology widely used in the industry using field-effect transistors. Another advantage of CMOS switches is possibility of their integration on the same semiconductor die with other components of the electronic devices.

The most typical topology used in CMOS switches is a λ/4 shunt [4]–[9]. It uses a quarter wavelength sections of transmission lines as impedance transformers (fig. 1). In this topology input terminal of the switch is connected to two branches with quarter-wave transmission lines. Between the ends of these lines and switch outputs the transistors are connected between line and ground. When the transistor is in the on-state, it lowers the impedance at the end of the λ/4 line which is transformed to high impedance at the input. That isolates this branch of the switch. On the opposite branch the transistor stays in off-state and it is matched to line's characteristic impedance with parallel stub made from another section of transmission lines. This topology is widely used in most of the available RF switches. However there are significant drawbacks, especially for high frequency applications. The transmission lines used in this type of construction manufactured in semiconductor typically have high losses due to lossy substrate and also occupy large area on the chip. Another problem is a tradeoff between isolation and bandwidth. As the isolation is dependent on the low impedance of the transistor in the on-state, wider transistors are required. On the other hand increasing the transistor width increases it's off-state equivalent capacitance which decreases the available bandwidth. Shunt switches using 90nm process presented in [4] allows to achieve insertion loss level of below 1.9 dB and isolation better than 25 dB in 50-70 GHz. The 65 nm process allowed to achieve slightly better performance as shown in [5] and [6] with insertion loss less than 1.6 dB in 0-94 GHz band and less than 3.6 dB in 110-170 GHz band. Isolation of 19-32 dB and over 19.5 dB was achieved in the respective bands.

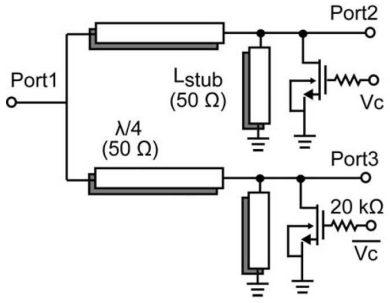

FIGURE 1. Schematic diagram of an SPDT switch with shunt topology [4].

The Silicon-On-Insulator CMOS (CMOS SOI; fig. 2) implementation for mm-wave shunt switches was also reported [8] which can be used to achieve better performance of CMOS switches at higher frequencies with insertion loss less than 1.5 dB and isolation around 20 dB in 140 - 220 GHz band. Another COMS SOI shunt switch implementation presented in [9] allowed to achieve better isolation (26.5 - 32 dB in 110-170 GHz band) but at the expense of higher insertion loss from 4 to 5 dB. A distributed switch with 4 shunt stages was also reported in SOI technology [10]. It exhibits high operation bandwidth from DC to 220 GHz with high isolation (30 - 50 dB) and moderate insertion loss (< 3.1 dB).

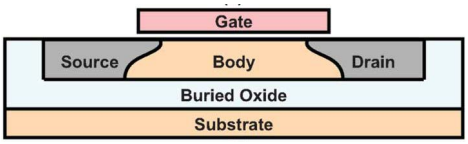

FIGURE 2. Cross-section of the transistor in a CMOS SOI process [8].

Another proposed topology for the mm-wave switches is a travelling-wave switch [11]–[13]. This topology (fig. 3) is similar to shunt switches and also uses sections of transmission lines. These highly inductive sections of transmission line are loaded by transistors. Several stages of this structure are used to obtain periodically loaded inductive transmission line. In the off-state of the transistors, their capacitance loads the inductive line to provide impedance matching which allow transmission (''artificial transmission line''). When transistors are in the on-state, the signal path is shorted to ground through their on-state resistance. The quarter-wave impedance transformer is added to the input side of the switch to transform short into open.

Application of travelling-wave switch concept in CMOS devices allowed to achieve higher isolation (over 27 dB in 50-94 GHz band [11] and over 40 dB in 70-110 GHz band [12]; fig. 4) compared to λ/4 shunt technique. These switches also offer higher power handling capabilities compared to other CMOS devices (IP1dB > 15 dBm). However their insertion loss is higher with below 3.3 dB in [11] and below 3.4 dB in [12]. Similar results for this type of structure can be also found in [13].

Further development of travelling-wave distributed switch with coupled inductors instead of transmission line sections was proposed in [14] which allowed to increase the isolation to over 33 dB in 54-84 GHz range and simultaneously decrease the insertion loss to below 2.5 dB also offering smaller occupied wafer area. This type of distributed switch was also reported in CMOS SOI [10] with very high operation bandwidth (DC - 220 GHz) and good insertion loss and

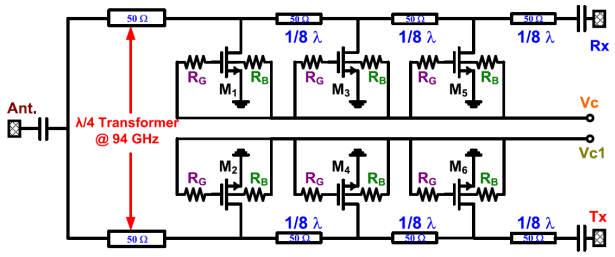

FIGURE 3. Schematic diagram of an SPDT switch with travelling-wave topology [12].

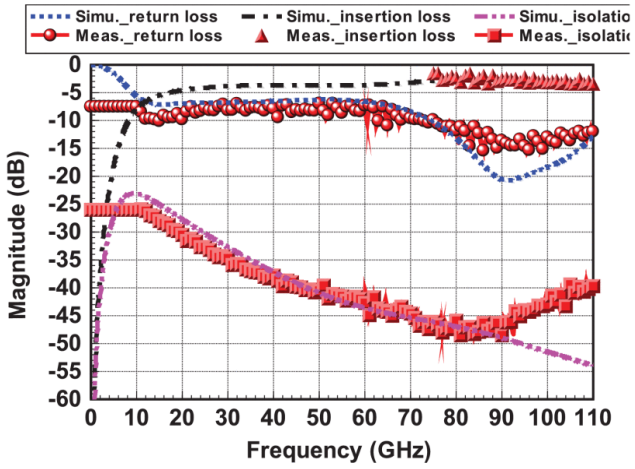

FIGURE 4. Scattering parameters of CMOS based SPDT switch with travelling-wave topology [12].

isolation characteristics (<3.1 dB and >37 dB, respectively in 60-220 GHz band).

Another two topologies presented for CMOS switches employ artificial resonator [15] and hybrid coupler [16]. First of them uses three coupled transmission lines (fig. 5). The one in the center is connected to input port and grounded on the opposite side. Two lines on the sides are connected to output ports and shunt transistors. When one of the transistors is in on-state, the line is shorted and port connected to it is isolated. At the same time the second transistor is in the off-state and it's parasitic components with coupled lines form artificial resonant network with bandpass transmission response from input to coupled output. This type of switch exhibits similar performance in terms of insertion loss (3.5-4 dB in 130-180 GHz band) and isolation (22-23 dB) to λ/4 shut switches, but offers significantly smaller occupied wafer area. It is also one of the fastest published CMOS switches in this frequency range with switch time around 580 ps.

Another example of a CMOS switch using coupled transmission lines can be found in [17]. This device operates in higher frequency range (290-320 GHz) with relatively high 5-7 dB insertion loss and high isolation around 40 dB. Results for both examples shows that the main drawback of coupled line based designs is narrow operation bandwidth.

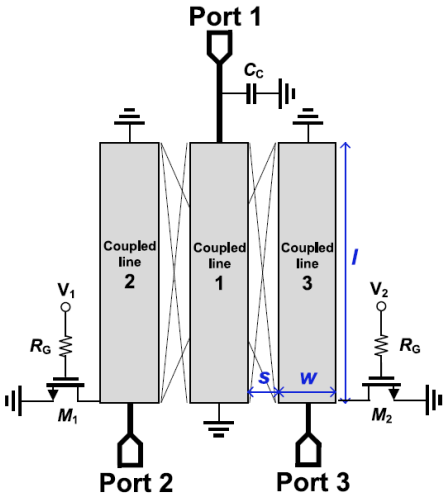

FIGURE 5. Schematic diagram of an SPDT switch with artificial resonator topology [15].

In [16] the concept of using 90° hybrid coupler with direct and coupled ports loaded with shunt transistors to achieve a SPST switch (fig. 6). It offers small occupied area, but its performance is inferior compared to other published CMOS mm-wave switches.

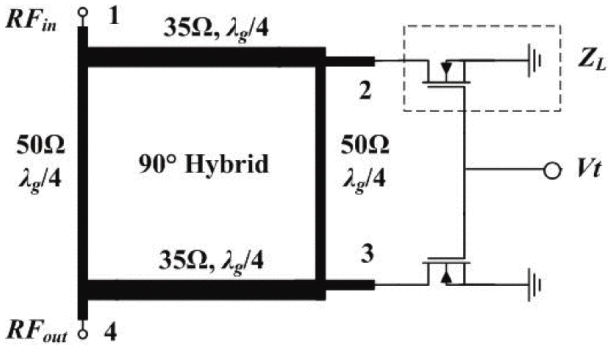

FIGURE 6. Schematic diagram of an SPDT switch using 90° hybrid coupler [13].

Among CMOS-based devices, there are also commercially available switches for mm-wave region. However their operating frequency is currently limited to about 60 GHz. An example of such device is PE42525 SPDT switch with operating frequency range from 9 kHz to 60 GHz [18]. It offers insertion loss below 3dB and isolation better than 35 dB in whole operating range.

One of the important limitations of all silicon CMOS devices is the low voltage operation which limits their power handling capabilities (maximum reported IP1dB around 15 dBm). Increasing transmitted power requires higher bandgap III - V semiconductors.

B. SiGe HBT

Another semiconductor technology proposed for mm-wave switches is using silicon-germanium (SiGe) substrates on

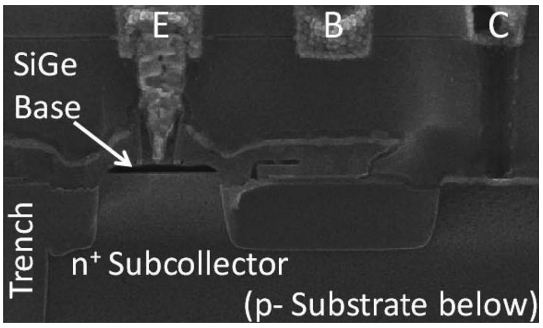

FIGURE 7. SEM Image of SiGe HBT transistor [21].

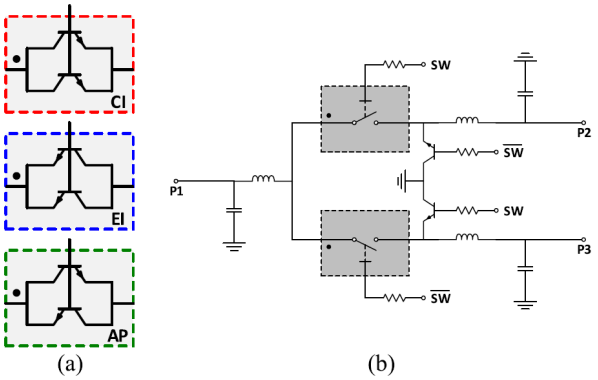

FIGURE 8. Proposed SPDT switch utilizing SiGe HBTs. (a) Three configurations of a series switch using SiGe HBT. (b) Schematic of the proposed SPDT switch. One of configurations in (a) replaces the black boxes. Anti-parallel (AP) configuration shows best performance [24].

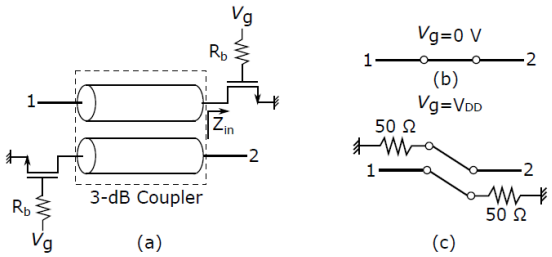

FIGURE 9. a) Schematic design of the through-load switch. Transistors are connected to the coupled ports of the coupler. b) Function of the device when $V_g = 0$. c) Function of the device when $V_g = VDD$ [25].

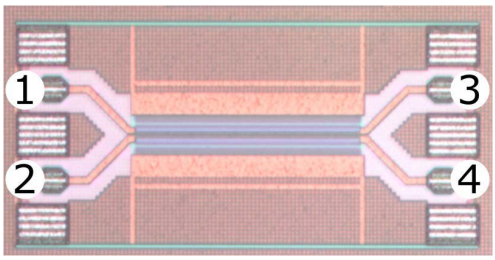

FIGURE 10. Micrograph of the fabricated coupler-based switch [25].

which heterojunction bipolar transistors (HBT) can be fabricated. This type of transistors allowed for decrease of the parasitic components and increase the transition frequency compared to silicon CMOS technology. It also offers better power handling capabilities still allowing high level of integration and low manufacturing costs.

Similarly to CMOS devices most SiGe mm-wave switches employs $\lambda/4$ shunt topology. SiGe HBT transistors (fig. 7) with less parasitic components allow decreasing the insertion loss compared to CMOS switches. Shunt switches shown in [19]–[21] offer lowest insertion loss values in mm-wave range among SiGe devices and noticeably better than CMOS devices at less than 1.25 dB in lower frequency band (42-70 GHz) [19] and between 1.1 dB and 1.5 dB in 75-100 GHz band [20], [21]. Isolation of these switches is comparable with CMOS devices (18-22 dB). The highest isolation in SiGe shunt switches was achieved in [22] and [23] (21-29 dB [22] and 26-31 dB [23] in 80-170 GHz and 110-170 GHz bands, respectively), however this values are still comparable with CMOS, and these devices exhibit higher insertion losses in the 2.6-4.5 dB range.

It should also be noted that SiGe shunt switches can achieve significantly faster operation (75 ps in [19]) and also higher power handling capabilities compared to CMOS switches (IP1dB = 35 dBm in [20]).

Better performance with simultaneously higher isolation, lower insertion loss as well as operation from DC can be achieved in SiGe using series-shunt topology (fig. 8) proposed in [24]. This type of switch utilizes three transistors. Two of them, in anti-parallel configuration form a series switching element which is followed by single shunt transistor. In this configuration insertion loss of 1.3-3.2 dB and isolation of 20-40 dB in 0-110 GHz frequency range was achieved. Presented device also exhibits fast switching time of under 250 ps.

Other notable SiGe device topology is a through-load switch (fig. 9, 10) proposed in [25]. This two-port device can switch between two states: a through connection or a 50 Ω load for both of its ports. It uses a 3 dB directional coupler composed with coupled lines and a two transistors connecting coupled ports to ground. In the off-state transistors represent high impedance at coupled ports which causes low loss transmission between remaining ports. In the on-state of the transistors represent impedance close to 50Ω obtained by optimization of transistor size. In such case the signal is dissipated in the transistors and ports are isolated. This configuration allowed to achieve good performance (1.4-2.2 dB insertion loss and 20-30 dB isolation) and also a low occupied wafer area of 0.019 mm^2.

SiGe HBT switches operating at higher frequencies (220-280 GHz) based on resonator topology was also reported [26]. These devices are constructed similarly to CMOS devices presented in [15] and achieve isolation comparable with SiGe switches for lower bands, however the insertion loss is significantly higher (4.2-5.3 dB insertion loss and 14-29 dB isolation).

C. InP DHBT

Next semiconductor technology for mm-wave switching is a InP double heterojunction bipolar transistor (DHBT) [27]–[31]. This type of transistor has heterojunctions at both emitter-base and base-collector junctions. It allows to obtain high frequency operation, low base-collector capacitances and fast switching with higher breakdown voltage than single heterojunction HBT's.

The InP DHBT for the 90-170 GHz reported in [27] uses double λ/4 shunt topology. It achieves significantly better isolation (>45 dB) compared to CMOS and HBT devices, but at the cost of slightly higher insertion loss than CMOS. The power handling capabilities are similar to both previously mentioned technology. This technology is suitable for integration and offers good performance with low power consumption and moderate costs.

Devices operating at higher frequencies were also presented in InP DHBT [28]–[31]. First of them [28] is a typical λ/4 shunt construction operating in 220-325 GHz frequency range. It offers insertion loss under 4.1 and high isolation of around 35 dB. It also exhibits higher power handling capability compared to most CMOS and HBT devices with IP1dB >20 dBm. Similar insertion loss (3-6 dB) with higher maximal isolation figures (up to 50 dB in 90-325 GHz range) was reported in [29]. Lower insertion loss shunt devices were also reported (1.2 - 2.9 dB), however with significantly lower isolation (13.1-15.7 dB) [30]. Another notable device [31] uses amplifier topology and offers slightly lower insertion loss under 4 dB and also lower isolation over 20 dB. However it is optimized for high speed operation with switching times around 40 ps which shows significant improvement over CMOS and HBT technologies.

It should also be noted that published InP DHBT transistor switches occupy significantly higher wafer areas (0.95 and 0.536 mm^2 for [27] and [28], respectively).

D. GaN HEMT

Another semiconductor material used for mm-wave switching is a GaN [32]–[34]. It offers high bandgap and high thermal conductivity which makes it suitable for high power density devices. GaN high electron mobility field effect transistors (HEMT) achieve transition frequencies and noise figures comparable to other semiconductors such as SiGe, InP or GaAs while at the same time their breakdown voltages are around five times higher.

GaN λ/4 shunt switch proposed in [32] offers lower insertion loss (0.9 - 1.4 dB in 60-110 GHz frequency range) compared to all previously considered technologies with high IP1dB over 27 dBm. However its isolation is very low, over 9 dB in whole band. In [33] isolation was improved to values comparable with SiGe. Semiconductor die image of this λ/4 shunt switch is shown in fig. 11.

In [34] slightly modified λ/4 shunt topology was used to achieve improved performance compared to CMOS, HBT and DHBT transistors in wide frequency range

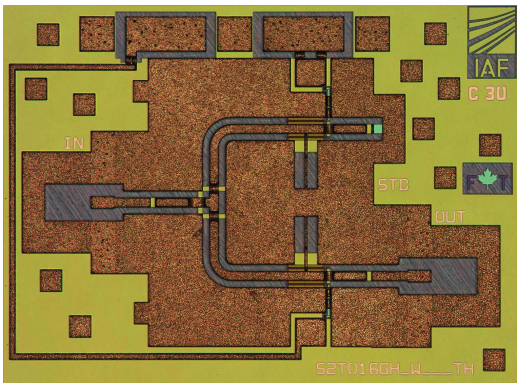

FIGURE 11. Microphotograph of GaN HEMT switch MMIC [33].

from 90 to 200 GHz. This device exhibits insertion loss form 1.8 dB to 3.2 dB and high isolation from 27 dB to 38 dB (fig. 12), and at the same time it is suitable for high power operation with IP1dB over 33 dBm (fig. 13).

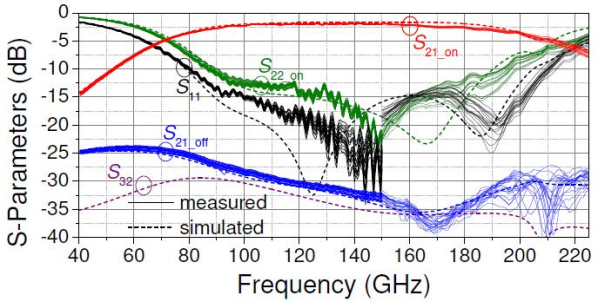

FIGURE 12. Scattering parameters of GaN HEMT based SPDT switch [34].

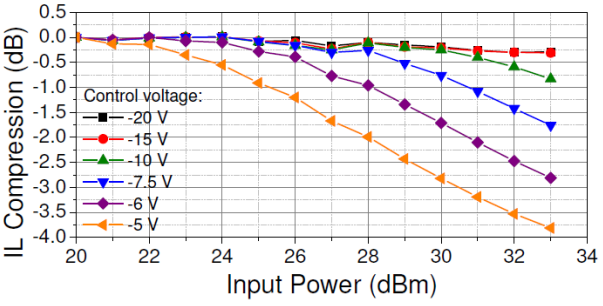

FIGURE 13. Insertion loss compression versus input power characteristics of GaN HEMT based SPDT switch [34].

Similarly to InP DHBT's, presented GaN HEMT transistors occupy large wafer area from 0.3 to 1.5 mm^2.

E. GaAs HEMT

Another semiconductor suitable for construction of HEMT transistors is GaAs. This semiconductor material exhibits high resistivity which leads to lower both parasitics and losses. At the same time it is suitable for high transition frequency transistors.

Among the highest performance switches in GaAs travelling wave and shunt topologies are present [35]–[37]. Travelling wave switch shown in [35] exhibit low insertion loss under 2 dB and isolation over 30 dB which is comparable with state of the art CMOS and HBT devices in the same frequency range (48-85 GHz). In [36] another travelling wave switch is presented with wider operation frequency range (0-135 GHz), insertion loss (<1-5 dB) comparable to CMOS and HBT devices and improved isolation in 16-45 dB range.

In [37] device exhibiting lower insertion loss than in previously considered technologies (under 1.1 dB in 59-77 GHz range compared to [19] and [21]) with higher isolation over 25 dB. This device uses modified travelling-wave topology with transistors integrated with CPW transmission line (fig. 14, 15).

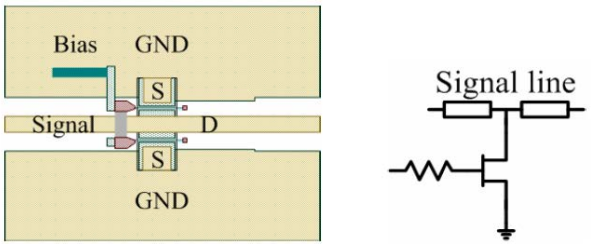

FIGURE 14. Layout and the equivalent circuit of FET integrated CPW line [37].

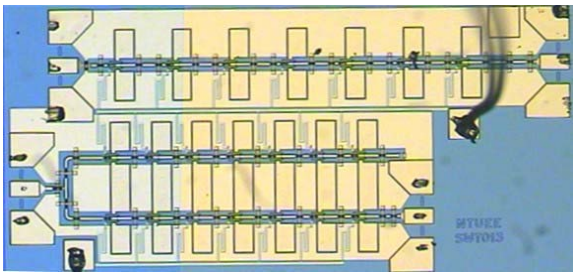

FIGURE 15. Die photograph of SPST and SPDT switches based on HEMT transistors integrated with CPW transmission line [37].

F. InGaAs mHEMT

To avoid creation of deep level traps in heterojunction HEMT devices, buffer layer in the junction is added creating a metamorphic HEMT (mHEMT). In InGaAs metamorphic transistors are constructed with GaAs substrate, AlInAs buffer layer and InGaAs channel. This construction also allows to optimize performance of the transistors by changing indium concentration in the channel [38].

There are multiple examples of the InGaAs mHEMT based switches for mm-wave frequency range [39]–[44]. Most of them are based on typical λ/4 shunt topology (fig. 16). In [39] a shunt switch operating in 53-150 GHz frequency range is presented. It achieves insertion loss under 3 dB which is only slightly higher than for state of the art SiGe HBT and GaN HEMT devices, but at the same time the isolation is

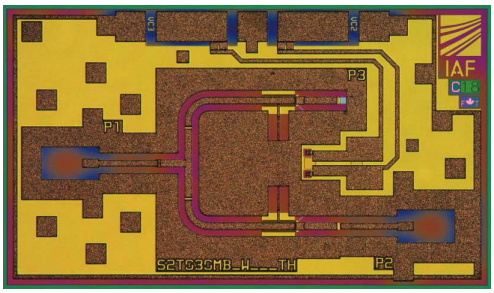

FIGURE 16. Microphotograph of InGaAs mHEMT switch MMIC [41].

significantly higher over 36 dB in whole operating frequency range. As shown in [40] the isolation figures can be further increased (to 35-52 dB in 52-168 GHz band and to 50-65 dB in 75-170 GHz band) at the cost of higher insertion losses (2.1-5.1 dB and 3-6 dB in respective bands). Lowest InGaAs mHEMT switch insertion loss in frequency range similar to aforementioned examples (1.0-1.9 dB in 72-120 GHz range) was reported in [41]. This device also exhibits higher isolation than HBT and GaN HEMT devices of comparable performance in terms of insertion loss. The power handling capabilities of these devices is also comparable to HBT switches (IP1dB around 19 dBm; fig. 17).

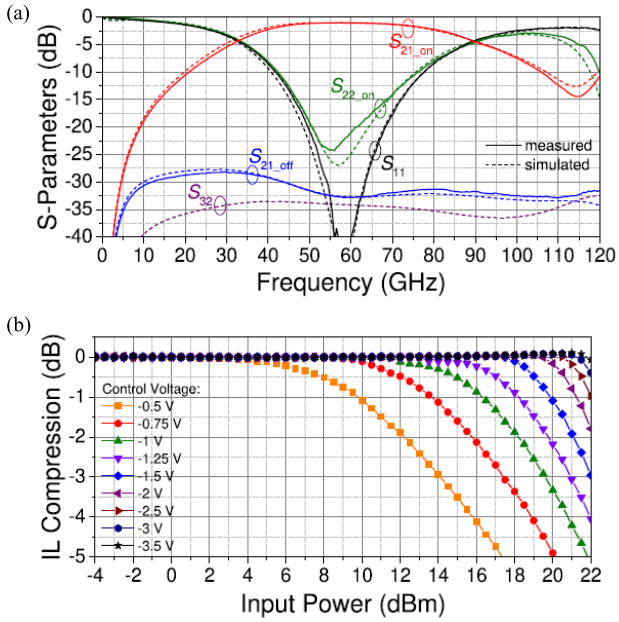

FIGURE 17. (a) Scattering parameters and (b) insertion loss compression characteristics of InGaAs mHEMT switch [41].

InGaAs mHEMT switches for higher operating frequencies were presented in [40] and [42]. In [40] the insertion loss of 1.5-4.5 dB and 13.5-22.8 dB isolation was reported in 122-330 GHz range. Switch presented in [42] operates in 200-330 GHz band with insertion loss in 1.7-5 dB range and isolation over 14 dB. As can be noticed, performance of these devices is only slightly worse compared to aforementioned

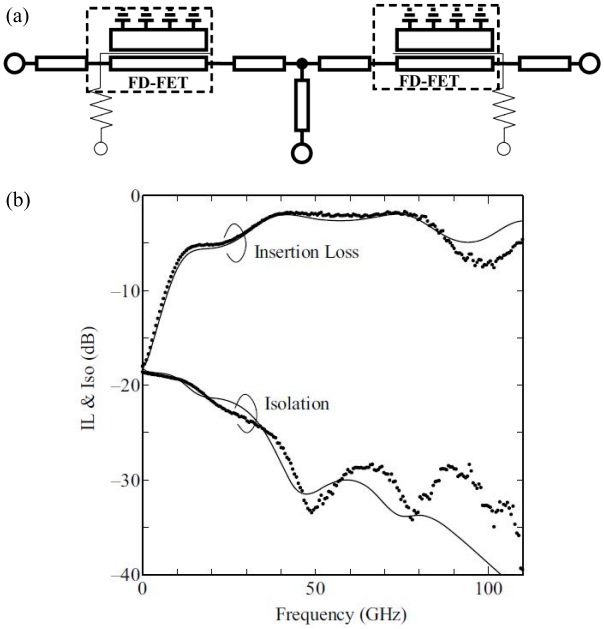

FIGURE 18. (a) Schematic diagram and (b) parameters of InGaAs mHEMT switch using travelling wave topology [43].

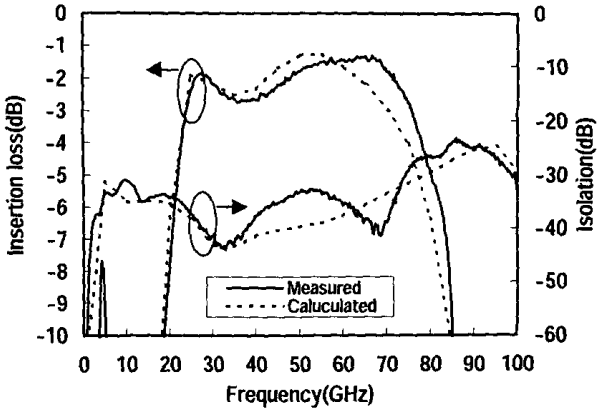

FIGURE 19. Parameters of InGaAs mHEMT switch using transistors in diode configuration in distributed shunt topology [44].

InP DHBT devices working in similar frequency range reported in [28] an [31].

Other noticeable topologies for InGaAs mHEMT switches were reported in [43] and [44]. Switch presented in [43] uses travelling wave topology (fig. 18) and achieves under 2.1 dB insertion loss and over 25.5 dB isolation in 38-80 GHz frequency range. These figures are comparable to the results achieved in CMOS devices.

It should be noted that transistors used in switching applications can also be used as active devices to amplify the switched signal [45]. Such devices can be used to compensate significant losses at high frequencies. The drawbacks of this approach are unidirectional operation of active switches and additional noise introduced by active circuit.

An interesting concept is presented in [44]. In this switch, the transistors are configured as diodes and used in distributed shunt configuration. The diodes created form HEMT transistors exhibit low Schottky capacitance and resistance lower than that of the transistor. Its resistance in still higher than PIN diodes, but it can be easily integrated into MMICs unlike PIN devices. The performance of this device is better than devices in other technologies mentioned before working in similar frequency range. Diode based switch exhibits 1.3-1.8 dB insertion loss and 32-41 dB isolation in 50-70 GHz with IP1dB of 20 dBm (fig. 19).

III. PIN DIODE SWITCHES

Besides transistors, there are other classes of devices available for mm-wave switching applications. First of them is a PIN diode. PIN diodes are widely used in RF switches due to their low parasitic capacitance, low series resistance and high power handling capabilities. There are also a significant drawbacks. First are different manufacturing requirements compared to transistors which are a major obstacle to integration of the PIN diodes into MMICs. Another weak sides of PIN diode switches are high control current requirements and high switching times.

PIN diode based switches reported in literature or commercially available typically use shunt topology and GaAs semiconductors [46]–[49]. In terms of insertion loss this type of switches can be comparable or slightly better than switches in other technologies presented earlier (1.1-1.6 dB in 75-100GHz range [46] and 0.75-2 dB in 85-105 GHz range [47]; fig. 20). However their isolation is moderate (over 21dB), and better overall performance can be achieved with InGaAs mHEMTs [41] with very similar insertion loss, but significantly better isolation. The IP1dB of the mentioned PIN switches was not reported, so possible advantages of PIN in power handling cannot be evaluated.

There are commercially available mm-wave switches based on GaAs PIN diodes. An Analog Devices HMC-SDD112 [48] is a 55-90 GHz SPDT shunt switch available as bare die. It offers insertion loss in 1.0-2.5 dB range and high isolation in 25-45 dB range (fig. 21). The power handling and switching speed specifications are not provided by the manufacturer. It should be noted that this device requires high control current of 22 mA at 5V.

Another examples of commercially available mm-wave PIN switches are HSW1001 and HSW1003 waveguide switches manufactured by HXI [49] (fig. 22). These devices working in 75-110 GHz range are optimized for low insertion loss (HSW1001) or high isolation (HSW1003). First offers under 2.2 dB insertion loss with over 18 dB isolation while second exhibits under 3.5 dB insertion loss with over 40 dB isolation (fig. 23). These switches are characterized by switch-on times (150 and 175 ns, respectively) significantly slower than switch-off times (25 and 30 ns, respectively). These switching times are one to two orders of magnitude larger than reported for state of the art transistor-based devices.

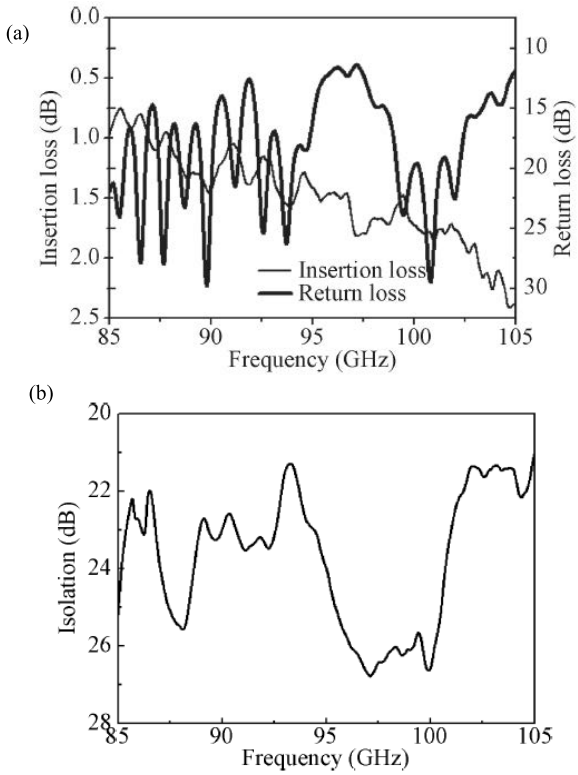

FIGURE 20. Measured (a) insertion, return loss and (b) isolation of GaAs PIN diode based SPDT switch for 85-105 GHz band [47].

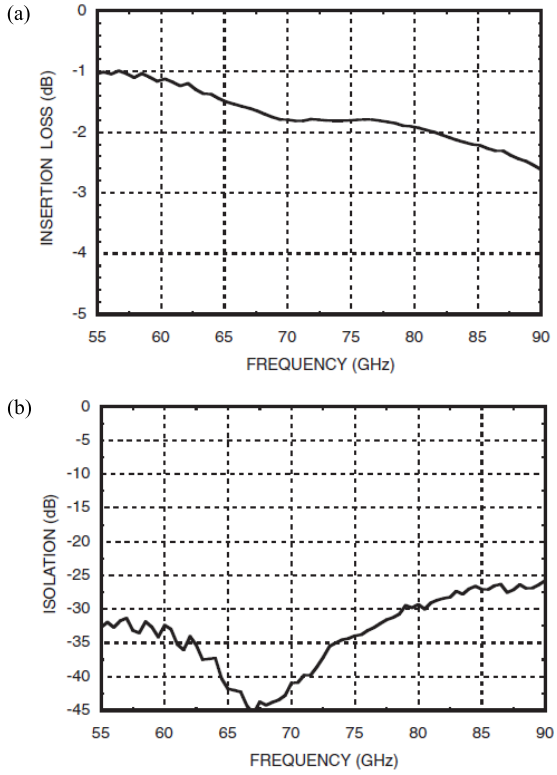

FIGURE 21. Typical (a) insertion loss and (b) isolation of commercially available PIN diode based SPDT MMIC switch HMC-SDD112 [48].

Typically, PIN diodes are not compatible with MMIC manufacturing technological processes which hinders their integration. However, as reported in [50] there are techniques that allow PIN diode construction using typical SiGe BiCMOS technology (fig. 24) widely used for MMICs. Presented device, with 77-133 GHz operating frequency range is based on typical $\lambda/4$ shunt topology. It offers performance comparable to SiGe HBT devices (1.4-2 dB insertion loss and 19-22 dB isolation), but with higher power handling capabilities (IP1dB over 24 dBm, with measurement limited by available source power).

Another special type of PIN diode which can be used in mm-wave switching applications is a surface PIN diode (S-PIN). Contrary to typical PIN diodes, the S-PIN structure is lateral. It creates an area, which conductivity can be controlled by external bias. So far most reported S-PIN devices are waveguide based [51], [52] but the construction of the S-PIN diodes allows to use them also in planar transmission lines. As shown in [51], [52] this type of switching element can be integrated into mm-wave antenna arrays to obtain beam steering. The reported devices use S-PIN diodes manufactured using SOI technology to create reconfigurable radiating slots in the waveguide. Such antenna array can achieve $\pm$ 45° beam steering range [51]. As the S-PIN switches are integrated with antennas, their insertion loss and isolation are not provided. In [52] switching speeds of 10 - 20 μs are reported, which allowed for time-modulated

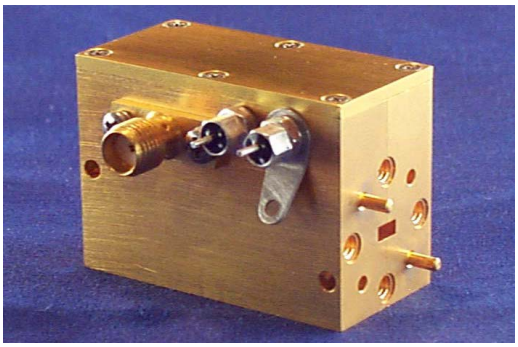

FIGURE 22. Commercially available PIN diode based W-band waveguide switch HSW1003 [49].

antenna array construction. An important drawbacks of the S-PIN are high power consumption and requirements for bipolar bias voltage.

IV. MEMS DEVICES

Another class of mm-wave switches are microelectromechanical system (MEMS) based devices. The construction of most of the high frequency MEMS switches is based on the shunt topology [53]–[60]. In the off-state of the switch, the transmission line (typically coplanar weveguide) is shorted by a conductive membrane. Therefore the reflective switches are typical for MEMS. The membrane of the MEMS switch is actuated electrostatically thus the required control voltage

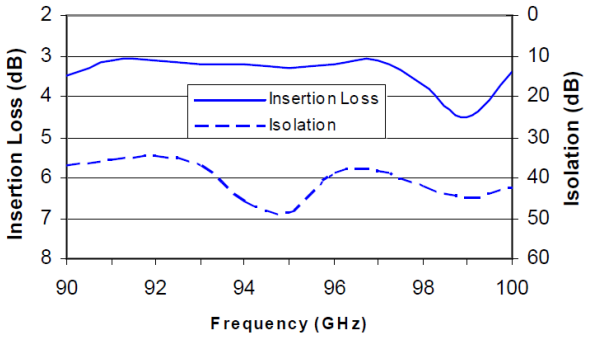

FIGURE 23. Typical parameters of commercially available PIN diode based W-band waveguide switch HSW1003 [49].

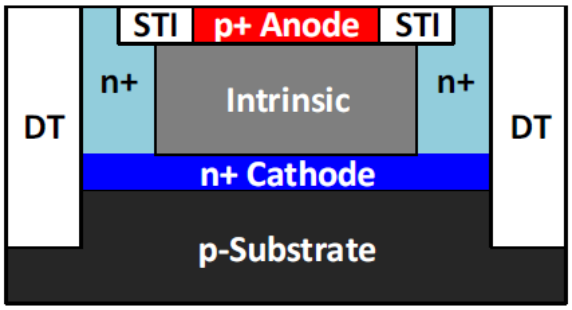

FIGURE 24. Cross-section of a vertical SiGe PIN diode suitable for integration in SiGe BiCMOS process [50].

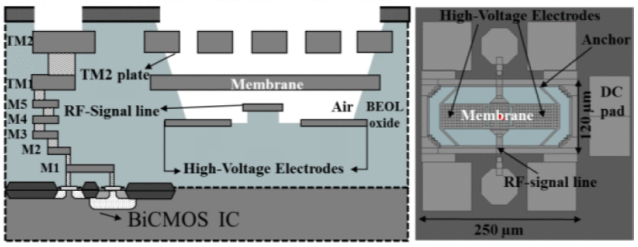

FIGURE 25. Construction details of MEMS – based SPST switch integrated in BiCMOS technology [56].

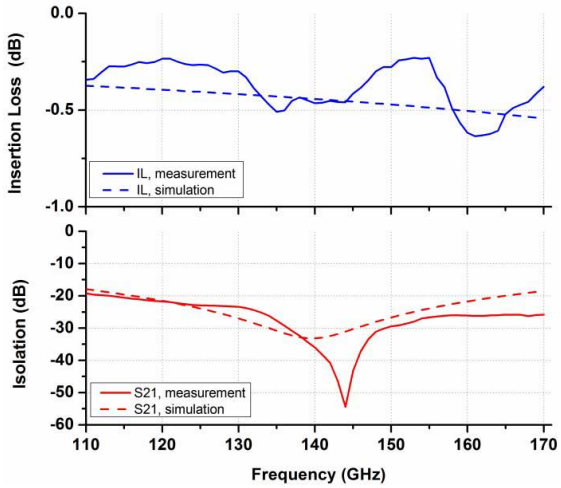

FIGURE 26. Simulated and measured parameters of BiCMOS MEMS SPST switch [56].

is significanly higher (45-60 V [53], [58]) than in semiconductor based devices. It should be noted that control voltage for the MEMS can be significanly reduced with apropriate construction of the device. MEMS RF switches operating up to 60 GHz with actuatiuon voltage of 6 V were reported in [60]. Their RF performance is comparable with other MEMS devices with under 0.7 dB insertion loss and isolation in 20 - 50 dB range in 30 - 60 GHz band. Such devices can be a suitable for 5G applications. An interesting obsevation shown in [60] is that actuation voltage increases with operating temperature of the switch.

Membranes are typically made of metal but other conductive materials such as graphene are also possible [61]. MEMS devices used to be very difficult and expensive to integrate within MMICs due to complicated and incompatibole manufacturing processes. Nowadays MEMS - based switches were reported using typical IV group semiconductor materials [53]–[59]. They can be produced with processes compatible with other MMIC building blocks [54], [56] (fig. 25). It is also possible to use MEMS devices in waveguide switches [58], [59] (fig. 27).

Due to low parasitics, these devices can achieve very low insertion losses, significantly better than transistor or PIN diode based switches in the similar frequency range (under 0.8 dB in 0-67 GHz range [53]; 0.8-1 dB in 70-110 GHz range [55] and 1.23-1.68 dB in 110-170 GHz range [56]; fig. 26). At the same time isolation is comparable (over 20 dB in [62] and 20-30 dB in [55]) or better (18.25-54.5 dB in [56]). Devices operating at higher bands (220-325 GHz in [57]) were also reported with slightly higher insertion loss and lower isolation (under 1.1 dB and under 24 dB, respectively). MEMS devices can also work in high temperatures and provide high power handling capabilities. The main drawback of the MEMS switches is slow switching speed (in order of 10 μs [58]). In some applications such as time-modulated systems slow switching speed is main obstacle for using MEMS switch.

V. PHASE-CHANGE MATERIALS

An interesting class of mm-wave switches are devices using phase-change material (PCM). These devices typically utilize two materials: germanium telluride (GeTe) and vanadium dioxide (VO2) [62]–[68]. Aforementioned PCM materials are thermo-chromic, i.e. change their states between conductor and insulator under influence of heat. GeTe is a material widely used in the industry for manufacturing of optical storage media (CD, DVD) which leads to low cost and high availability. It has unique properties which allows creation of latching switches which require power only during switching time. As reported in [62] these times can be as low as 2 μs which is almost an order of magnitude faster than comparable performance MEMS devices (fig. 28, 29).

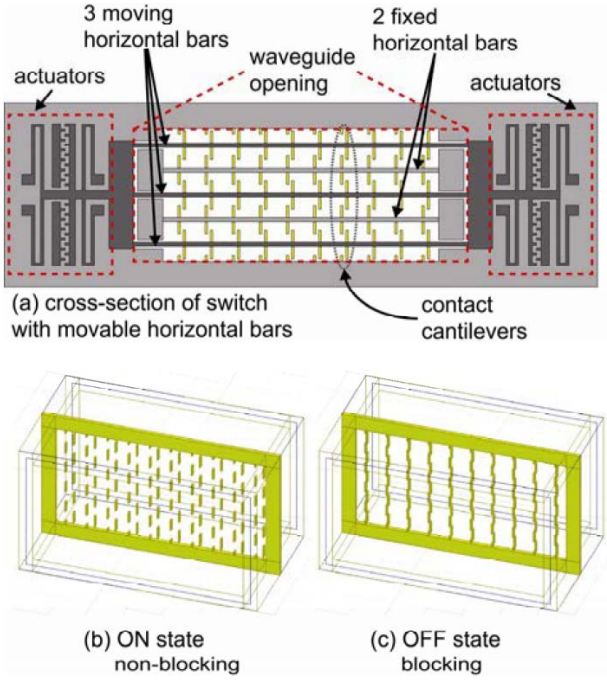

FIGURE 27. Construction of MEMS – based WR-12 waveguide SPST switch [59].

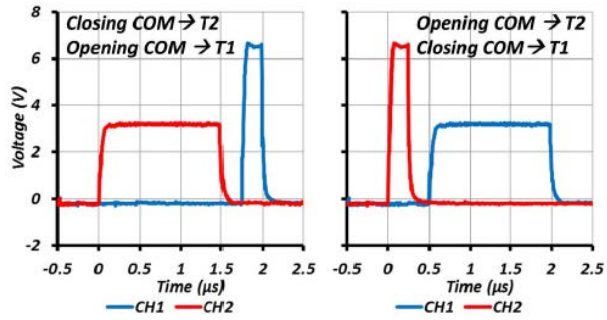

FIGURE 28. Switching waveforms for changing states of the GeTe - based switch [62].

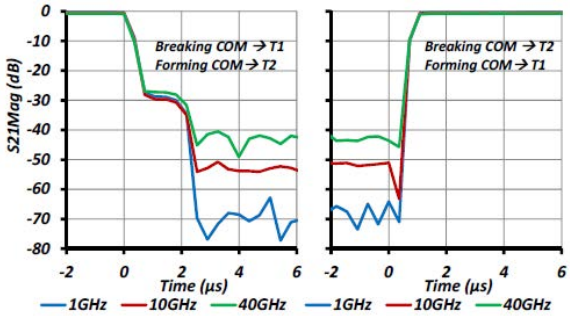

FIGURE 29. Transient RF response of GeTe – based switch during application of switching waveforms [62].

Till now, GeTe switches with operating frequency range up to 67 GHz were reported [62]–[65]. As shown in [55] and [56] this type of device offers very low insertion loss

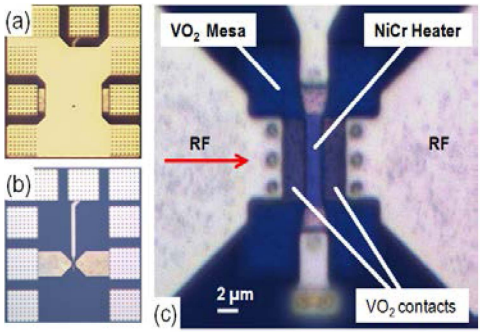

FIGURE 30. (a) Top view of the VO2 - based switch test structure. GSG probe pads are provided for RF as well as for heater bias. (b) and (c) Views of the switch prior to top metal deposition [67].

(under 1.1 dB in [55] and under 0.6 dB in [56]) as well as high isolation (over 39 dB in [55] and over 24 dB in [65]). GeTe switches can also achieve high power handling capabilities (i.e. 35.5 dBm in [65]).

Reported PCM based switches with higher operating frequencies utilize VO2 [66], [67]. This material does not have latching properties and requires constant 20 mW of heat in on-state. In [58] VO2 PCM based switch operating in 1-110 GHz frequency range was presented (fig. 30). It offers very low insertion loss under 0.6 dB, only comparable with MEMS devices and also good isolation between 15 and 45 dB (fig. 31). The switching time around 2 μs is comparable with GeTe based device.

Even higher operating frequency (210-290 GHz) for VO2 based device was reported in [67]. This device also offers very low insertion loss (0.5-1.5 dB), but with moderate isolation (11-20 dB).The switching time for this device equals 10 μs. An important advantages of PCM switches are also high power handling capabilities (IP1dB over 30 dBm in [67]) and small size. The main drawbacks are significant power consumption (in case of VO2 material) and non-standard process which is not directly compatible with typical MMIC technologies. However some integration possibilities have been reported [68].

VI. 2D MATERIALS

A special class of materials which is of great interest for many diverse applications in electronics is two-dimensional (2D) materials. 2D material is a special atomically-thin form of matter which properties differs from bulk material of the same composition. Some of these materials exhibit features which can be utilized in construction of high frequency devices. The development of the 2D material based RF devices is still at the early stage, thus not many mm-wave devices were reported and their operation frequency is mostly below 100 GHz.

A. MoS_2 MONOLAYERS

One of the 2D materials proposed for mm-wave switches is molybdenum disulfide (MoS_2). This material, commonly known as lubricating agent is a semiconductor which can be

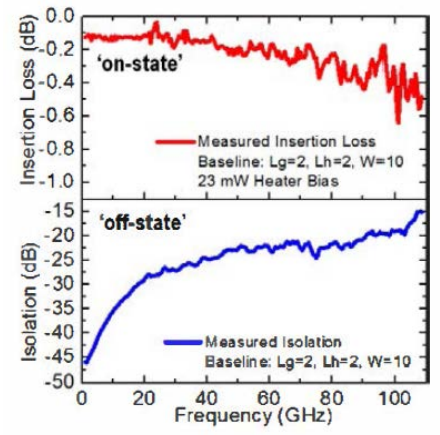

FIGURE 31. Measured transmission properties of the VO2 - based SPST switch. The red trace represents the on-state performance at 23 mW of heater power while the blue trace was produced with zero heater current (off-state) [66].

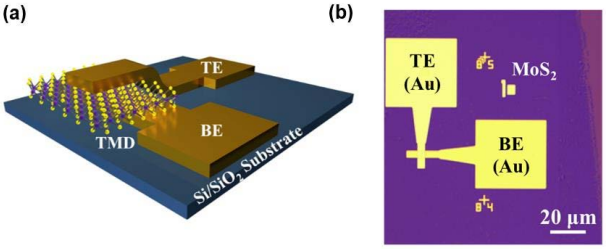

FIGURE 32. (a) Schematic illustration of vertical structure of a MoS2 switch. (b) Top-view optical image of a fabricated MoS2 switch with Au electrodes [69].

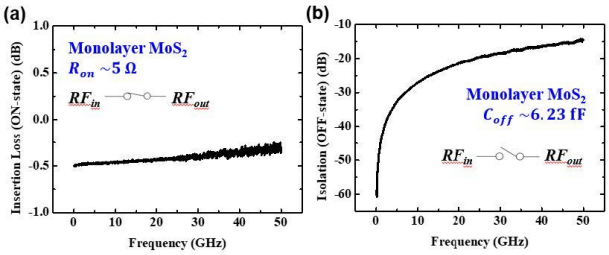

FIGURE 33. (a) Schematic illustration of vertical structure of a MoS2 switch. (b) Top-view optical image of a fabricated MoS2 switch with Au electrodes [69].

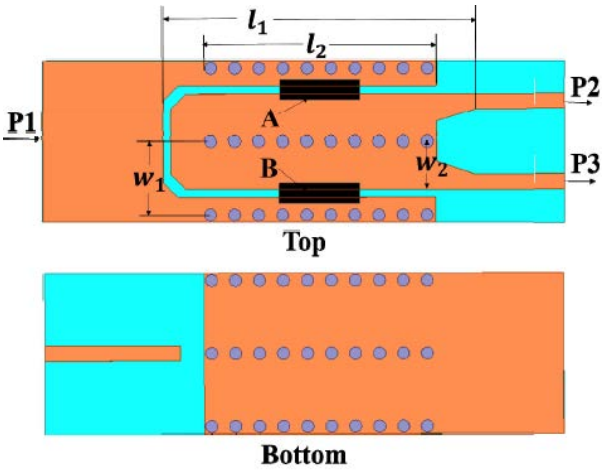

FIGURE 34. Schematic illustration of slotted substrate integrated waveguide based graphene SPDT switch [70].

deposited in atomically thin monolayers. MoS_2 monolayers exhibit high direct bandgap which makes them suitable for transistor construction (fig. 32).

An monolayer MoS_2 RF switch with 0-50 GHz operating frequency range was reported in [69]. It offers very low insertion loss (under 0.5 dB) compared to other transistor-based devices as well as PIN diodes (fig. 33). The isolation figures are moderate in 15-50 dB range. These figures show that even on the early stage of development MoS_2 switches exhibit competitive performance to more mature semiconductor devices. Therefore further research is required to investigate the capabilities of MoS_2 and improve the construction of the switches.

B. GRAPHENE

Graphene is a novel form of carbon which can form 2D layers. Despite its low thickness graphene retains good thermal and electrical conductivity of carbon which makes is suitable for electronic devices. An interesting property of graphene nanolayers is the ability to change their conductivity with external voltage. Due to this phenomenon graphene is considered for switching applications. There are several publications that analyses the possibilities of graphene-based RF switches for millimeter-wave band [61], [70]–[77]. However, most of these papers include only theoretical background and simulation results of such structures. Additionally operating frequencies of presented switches are below 100 GHz. Among aforementioned publications several different switch designs is shown. In [70] a design of SPDT switch based on slotted substrate integrated waveguide is presented (fig. 34). The simulated results that the proposed device exhibits better than 3 dB insertion loss and 17 dB isolation from 59.5 GHz to 60.8 GHz.

Another design developed for 60 GHz band and based on coplanar waveguide (CPW) with graphene layers between conductors (fig. 35) is presented in [71]. Simulation results shows insertion loss better than 5 dB and isolation between 32 dB and 45 dB in 20-70 GHz range (fig. 36). Similar construction (fig. 37) can also be found in [72].

Among very few experimentally examined graphene-based devices variable attenuators operating at the low end of the mm-wave range [73], [74] should be noted. The variable attenuators can be considered as a special type of the switch where there are multiple states between on-state and off-state. The device presented in [65] utilizes similar topology to the switches reported in [70]–[72] where voltage dependence of graphene resistance is used to change the state of the switch. This three-stage construction based on CPW operates

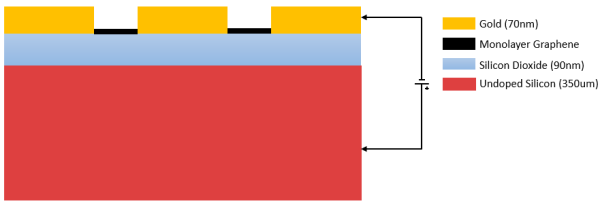

FIGURE 35. Schematic illustration of CPW-based graphene SPST switch [71].

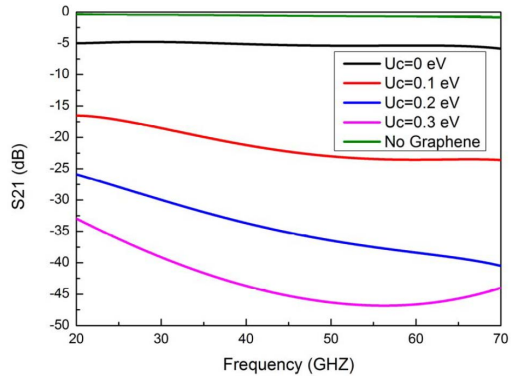

FIGURE 36. Simulated transmission characteristics of a CPW-based graphene SPST switch with different bias voltages [71].

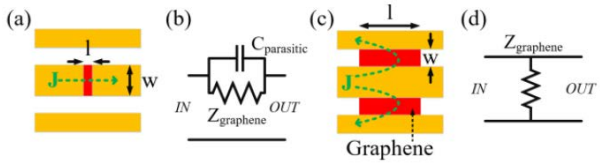

FIGURE 37. Schematic illustration of CPW-based graphene SPST switches [72].

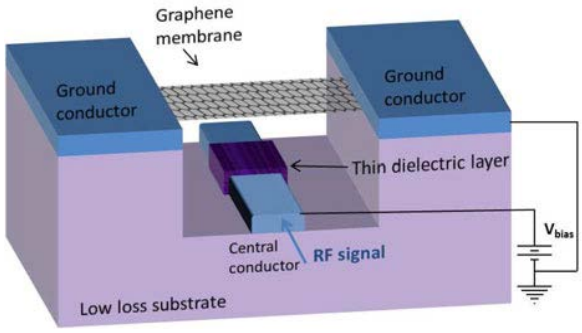

FIGURE 38. Schematic illustration of graphene-based RF NEMS switch [61].

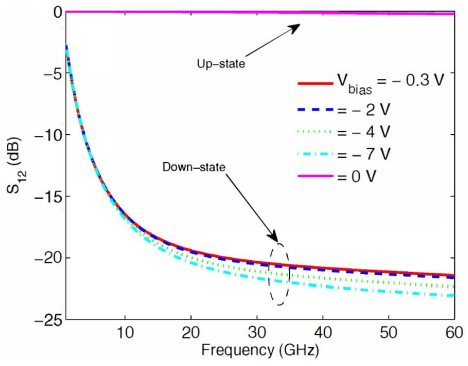

FIGURE 39. Simulated transmission characteristics of a graphene-based RF NEMS switch in two states with different bias voltages [8].

in 3.5-28 GHz frequency range with 2.5 dB insertion loss and 14 dB isolation. It should also be noted that this device exhibits high power consumption (390 mW) as the DC current flows through graphene elements.

In [74] two types of the variable attenuators for 10-40 GHz frequency range are examined. Both of them use variable resistance of grapheme element, first in CPW and second in slotline configuration. Contrary to construction reported in [73] one large two layer graphene element is used with additional insulating films. The insertion loss and isolation figures for both CPW and slotline attenuators are similar to those in [73] with 3 dB insertion loss and 15 dB isolation. However, application of insulating layers allowed for much better return loss characteristics of both deices (in the −20 to −40 dB range).

It should be noted that in these constructions the graphene layer itself is a switching element instead of being a part of semiconductor device. Another important characteristic of these devices is relatively high bias voltage (from 4 V in [74] to around 30 V [69], [71]) required to change state of the graphene layer.

Graphene layers can also be used to construct MEMS devices. This concept is investigated in [61], [75] and [76]. These structures are based on graphene nanolayer membrane suspended over specially constructed coplanar waveguide (fig. 38).

When bias voltage is applied the membrane bends and creates a short circuit in transmission line. The membranes can be constructed from either monolayer or multilayer grapheme. The simulations shows that with this design and multilayer graphene membranes it is possible to obtain insertion loss below 0.3 dB and isolation over 20 dB in 1-60 GHz frequency range (fig. 39). It should be noted that shown graphene-based MEMS devices require lower voltage to change state compared to typical metal-based MEMS switches.

Another concept for application of graphene in high frequency switching devices is a semiconductor device with grapheme monolayer used as a gate [77]. The reported device is based on AlGaN/GaN semiconductor structure similar to HEMT transistor embedded into a CPW with graphene layer used as a gate. The switch is constructed in series topology with switching device placed between two sections of CPW. In the on-state, without gate bias, the transmission occurs through two-dimensional electron gas channel at the AlGaN/GaN interface (fig. 40). When the graphene gate is

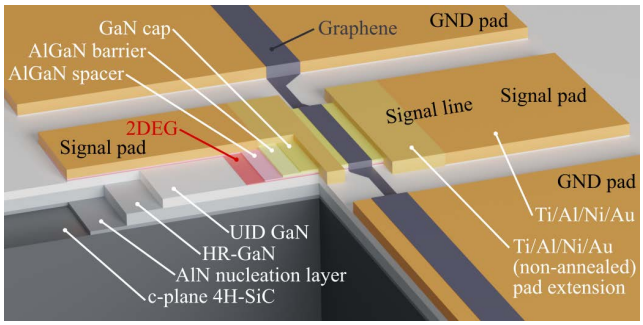

FIGURE 40. Structure of Graphene/AlGaN/GaN Switch [77].

polarized, it depletes the channel interrupting the transmission in CPW.

In contrast to typical HEMT transistors, bias voltage controls not only the conductivity of the channel but also the conductivity of the graphene gate. This property of graphene can be used to decrease the conductivity of the gate in the off-state. Therefore the parasitic coupling between two sides of the switch can be greatly reduced improving isolation. The switch reported in [77] operating in DC-84 GHz frequency range exhibits high isolation (17.5-77 dB), especially at low frequencies, but also very high insertion loss (7.4-19.4 dB). It also allows fast switching with rise and fall times of 25 ns and 17 ns, respectively. Considering the early stage of development of this type of switch and suboptimal design (i.e. series topology which typically introduces considerable losses) there is a room for improvement in high frequency performance. Fast operation and high low frequency isolation makes it a good candidate for further research on graphene-based switches.

If we consider a modulator as a switching device there is a considerable interest in application of graphene in optical modulators [78]. A significant number of publications on high-speed and high bandwidth devices operating in near infrared (around 1.5 μm/200 THz) can be found. However there are also reports of devices operating at frequencies as low as 200 GHz [79], [80]. As the devices are intended for operation in optical systems, they are configured for free-space incident beam modulation. Thus, they are impractical for application for typical mm-wave circuits. However it seems that straightforward adaptation for waveguide circuits is possible. Devices proposed in [79] and [80] are optically controlled which can be beneficial for some applications due to a fact that no electrical bias connections are required and they can be easily interfaced with optical communication systems. The principle of operation is similar for both reported devices. The active element of the modulator is a metamaterial created by deposition of graphene layer on a semiconductor plate. Device reported in [79] utilizes graphene on silicon (GOS) structure while in [80] graphene on germanium (GOG) is used. The metamaterial structure placed in the path of the mm-wave beam introduces very low attenuation without external excitation. In order to change the state of the modulator, the structure is illuminated with laser beam (40mW at 0.488 μm wavelength and 800 mW at 1.55 μm wavelength in [79] and [80], respectively). The carriers induced in the illuminated structure increase the conductivity and therefore attenuation of the mm-wave beam. The reported modulation depth can be as high as 99% for the GOS device operating in 0.2-2 THz range [79] and 94% for GOG device operating in 0.25-1 THz range. However, it should also be noted that modulation speed of these devices is very low at around 200 kHz [80].

VII. CONCLUSION

An overview of state-of-the-art mm-wave switches has been presented. Different manufacturing technologies as well as device topologies were considered in order to summarize their properties and compare performance. Additionally, novel unconventional solutions for mm-wave switching devices were highlighted.

The summary and comparison of the most important parameters of switches in different technologies as well as commercially available mm-wave devices is presented in Table 1. Considering transistor-based devices III-V semiconductor devices allow to achieve the highest operation frequency. However, advances in well-established CMOS technology enables operation of these devices up to 300 GHz. An important advantage of the CMOS devices is very straightforward integration with other circuits due to its prevalence in the industry. Therefore it can be used to create efficient, highly integrated system-on-chip solutions. The main drawbacks of CMOS are low power handling capability and slightly higher losses compared to other types of transistors. For high power applications switches based on GaN field effect or SiGe bipolar transistors can be used. In comparison with GaN transistors SiGe HBT's can achieve higher power handling, high speed switching, lower die size and cost, but at the expense of lower isolation figures. The highest switching speeds can be achieved in InP based solutions.

The PIN diodes, very common in microwave switches, can achieve similar loss, isolation and power handling performance to transistors but their operation frequency does not exceed 130 GHz. Moreover their low switching speed, large size and high power consumption combined with manufacturing process incompatible with MMICs makes them less attractive for mm-wave applications.

Among mm-wave switches there are also less conventional solutions compared with typical semiconductor devices. First of them is a MEMS, which allows to achieve significantly lower insertion losses than transistor based devices with comparable or higher isolation. Also the power handling capabilities of MEMS can be very high, although it is not reported for mm-wave devices. The main drawbacks of MEMS are very low switching speed, high control voltage requirements and complicated manufacturing process which hinders their integration. Another solution which allows to achieve very

TABLE 1. Comparison of state-of-the-art subterahrtz switches in different technologies.

Parameter	CMOS	SiGe HBT	InP DHBT	GaN HEMT	GaAs / InGaAs HEMT	PIN	MEMS	PCM	AD HMC-SDD 112	HXI HSW 1003	Gotmic gSSS0 015	Keysight TC950
Max. freq. [GHz]	300	250	320	310	330	130	240	300	90	110	110	75
Loss (>100 GHz) [dB]	1,5 - 7	1,4 - 4,5	1,2 - 5	1,4 - 3,2	1,5 - 6	1,5 - 3,5	0,45 - 2	0,6 - 1,5	1 - 2.5	< 3.5	< 3.5	< 4
Isolation (>100 GHz) [dB]	20 - 66	20 - 26	20 - 45	20 - 38	20 - 50	20 - 40	20 - 55	15 - 20	25 - 45	> 40	> 22	> 26
Switching time	> 550 ps	> 75 ps	> 50 ps	n/a	> 1.5 ns	> 30 ns	< 10 µs	2 - 10 µs	n/a	170 ns	>20 ps	< 1 ns
Max IP1dB	15	35	20	33	20	>24	n/a	>30	n/a	25	15	15
Die size	small	small	medium	medium	medium /large	medium/ large	large	small/ medium	large	n/a	large	large
Power consumption	low	low	low	low	low	high	low	moderate	110 mW	50 mW	0 mW	60 µW
Control voltage	low	low	low	low	low	moderate	high	moderate	± 5 V	+5 / - 15 V	-2 V	±3 V
Straightforward MMIC integration	Yes	Yes	Yes	Yes	Yes	No	No	No	n/a	n/a	n/a	n/a
Reference	[4 - 18]	[19 - 26]	[27 - 31]	[32 - 34]	[35 - 45]	[46 - 50]	[53 - 60]	[62 - 68]	[48]	[49]	[81]	[82]

low insertion loss similar to MEMS is application of phase-change materials. An important advantage of PCM is almost an order of magnitude faster switching compared to MEMS. On the other hand, the PCM switches exhibit significantly smaller isolation figures and high power consumption due to actuation by heat.

A solution for future mm-wave switches which brings considerable research interest is application of 2D materials such as MoS_2or graphene. Published results for MoS_2 devices operating at low end of mm-wave range shows performance competitive with typical semiconductor solutions, especially in terms of insertion loss. Therefore it is a promising technology for further research.

Graphene is a 2D material which diverse applications are a subject of great research effort in the last decade. However, mm-wave switching devices with graphene are on the early stage of development. Moreover, among investigated devices, very few were manufactured and experimentally evaluated. Most of the proposed solutions utilizes the phenomenon of graphene conductivity changes with applied voltage for controlling the attenuation in transmission lines. Graphene can be also used as a membrane in MEMS devices. Another proposed application of graphene in mm-switching is semiconductor device with graphene used as a gate. Reported performance of the first prototypes of such device shows very good isolation at low frequencies and low switching times. Therefore, it is a promising solution for further development and optimization.

REFERENCES

[1] R. B. Yishay and D. Elad, "Low power 75–110 GHz SiGe Dicke radiometer front-end," in *IEEE MTT-S Int. Microw. Symp. Dig.*, Jun. 2021, pp. 885–887, doi: 10.1109/IMS19712.2021.9575002.

[2] B. Ustundag, E. Turkmen, A. Burak, B. Gungor, H. Kandis, B. Cetindogan, M. Yazici, M. Kaynak, and Y. Gurbuz, "Front-end blocks of a W-band Dicke radiometer in SiGe BiCMOS technology," *IEEE Trans. Circuits Syst. II, Exp. Briefs*, vol. 67, no. 11, pp. 2417–2421, Nov. 2020, doi: 10.1109/TCSII.2020.2968313.

[3] M. Frounchi and J. D. Cressler, "A SiGe millimeter-wave front-end for remote sensing and imaging," in *Proc. IEEE Radio Freq. Integr. Circuits Symp. (RFIC)*, Aug. 2020, pp. 227–230, doi: 10.1109/RFIC49505.2020.9218399.

[4] M. Uzunkol and G. M. Rebeiz, "A low-loss 50–70 GHz SPDT switch in 90 nm CMOS," *IEEE J. Solid-State Circuits*, vol. 45, no. 10, pp. 2003–2007, Oct. 2010, doi: 10.1109/JSSC.2010.2057950.

[5] A. Tomkins, P. Garcia, and S. P. Voinigescu, "A 94 GHz SPST switch in 65 nm bulk CMOS," in *Proc. IEEE Compound Semiconductor Integr. Circuits Symp.*, Monterey, CA, USA, Oct. 2008, pp. 1–4, doi: 10.1109/CSICS.2008.34.

[6] U. Yodprasit, R. Fujimoto, M. Motoyoshi, K. Takano, and M. Fujishima, "D-band 3.6-dB-insertion-loss ASK modulator with 19.5-dB isolation in 65-nm CMOS technology," in *Proc. Asia–Pacific Microw. Conf.*, Yokohama, Japan, 2010, pp. 1853–1856.

[7] A. Tomkins, P. Garcia, and S. P. Voinigescu, "A passive W-band imaging receiver in 65-nm bulk CMOS," *IEEE J. Solid-State Circuits*, vol. 45, no. 10, pp. 1981–1991, Oct. 2010, doi: 10.1109/JSSC.2010.2058150.

[8] M. Uzunkol and G. M. Rebeiz, "140–220 GHz SPST and SPDT switches in 45 nm CMOS SOI," *IEEE Microw. Wireless Compon. Lett.*, vol. 22, no. 8, pp. 412–414, Aug. 2012, doi: 10.1109/LMWC.2012.2206017.

[9] W. T. Khan, A. C. Ulusoy, R. Schmid, T. Chi, J. D. Cressler, H. Wang, and J. Papapolymerou, "A D-band (110 to 170 GHz) SPDT switch in 32 nm CMOS SOI," in *IEEE MTT-S Int. Microw. Symp. Dig.*, Phoenix, AZ, USA, May 2015, pp. 1–3, doi: 10.1109/MWSYM.2015.7167061.

[10] L. Wu, H. Y. Hsu, and S. P. Voinigescu, "A DC to 220-GHz high-isolation SPST switch in 22-nm FDSOI CMOS," *IEEE Microw. Wireless Compon. Lett.*, vol. 31, no. 6, pp. 775–778, Jun. 2021, doi: 10.1109/LMWC.2021.3067003.

[11] S. Chao, H. Wang, C. Su, and J. G. J. Chern, "A 50 to 94-GHz CMOS SPDT switch using traveling-wave concept," *IEEE Microw. Wireless Compon. Lett.*, vol. 17, no. 2, pp. 130–132, Feb. 2007, doi: 10.1109/LMWC.2006.890339.

[12] W.-C. Lai, C.-C. Chou, S.-C. Huang, T.-T. Huang, and H.-R. Chuang, "75–110-GHz *W*-band high-linearity traveling-wave T/R switch by using negative gate/body-biasing in 90-nm CMOS," *IEEE Microw. Wireless Compon. Lett.*, vol. 27, no. 5, pp. 488–490, May 2017, doi: 10.1109/LMWC.2017.2690837.

[13] R.-B. Lai, J.-J. Kuo, and H. Wang, "A 60–110 GHz transmission-line integrated SPDT switch in 90 nm CMOS technology," *IEEE Microw. Wireless Compon. Lett.*, vol. 20, no. 2, pp. 85–87, Feb. 2010, doi: 10.1109/LMWC.2009.2038519.

[14] R. Shu, J. Li, T. Adrian, B. J. Drouin, and Q. J. Gu, "Coupling-inductor-based hybrid mm-wave CMOS SPST switch," *IEEE Trans. Circuits Syst. II, Exp. Briefs*, vol. 64, no. 4, pp. 367–371, Apr. 2017, doi: 10.1109/TCSII.2016.2565509.

[15] F. Meng, K. Ma, K. S. Yeo, and S. Xu, "Monolithic sub-terahertz SPDT switches with low insertion loss and enhanced isolation," *IEEE Trans. THz Sci. Technol.*, vol. 8, no. 2, pp. 192–200, Mar. 2018, doi: 10.1109/TTHZ.2017.2786024.

[16] X.-D. Deng, Y. Li, W. Wu, and Y.-Z. Xiong, "A W-band single-pole single-throw switch using on-chip rectangular coaxial transmission line in 0.13-μm CMOS technology," in *Proc. Asia–Pacific Microw. Conf. (APMC)*, Nanjing, China, Dec. 2015, pp. 1–3, doi: 10.1109/APMC.2015.7413200.

[17] J. Kim, S. Kim, K. Song, and J.-S. Rieh, "A 300-GHz SPST switch with a new coupled-line topology in 65-nm CMOS technology," *IEEE Trans. THz Sci. Technol.*, vol. 9, no. 2, pp. 215–218, Mar. 2019, doi: 10.1109/TTHZ.2019.2898815.

[18] *Peregrine Semiconductor PE42525 RF Switch Datasheet*. Accessed: Jan. 1, 2022. [Online]. Available: https://www.psemi.com/pdf/datasheets/pe42525ds.pdf

[19] M. Thian and V. F. Fusco, "Ultrafast low-loss 42–70 GHz differential SPDT switch in 0.35 μm SiGe technology," *IEEE Trans. Microw. Theory Techn.*, vol. 60, no. 3, pp. 655–659, Mar. 2012, doi: 10.1109/TMTT.2011.2180395.

[20] R. L. Schmid, A. C. Ulusoy, P. Song, and J. D. Cressler, "A 94 GHz, 1.4 dB insertion loss single-pole double-throw switch using reverse-saturated SiGe HBTs," *IEEE Microw. Wireless Compon. Lett.*, vol. 24, no. 1, pp. 56–58, Jan. 2014, doi: 10.1109/LMWC.2013.2288276.

[21] R. L. Schmid, P. Song, C. T. Coen, A. C. Ulusoy, and J. D. Cressler, "On the analysis and design of low-loss single-pole double-throw W-band switches utilizing saturated SiGe HBTs," *IEEE Trans. Microw. Theory Techn.*, vol. 62, no. 11, pp. 2755–2767, Nov. 2014, doi: 10.1109/TMTT.2014.2354017.

[22] A. Ç. Ulusoy, P. Song, R. L. Schmid, W. T. Khan, M. Kaynak, B. Tillack, J. Papapolymerou, and J. D. Cressler, "A low-loss and high isolation D-band SPDT switch utilizing deep-saturated SiGe HBTs," *IEEE Microw. Wireless Compon. Lett.*, vol. 24, no. 6, pp. 400–402, Jun. 2014, doi: 10.1109/LMWC.2014.2313529.

[23] B. Cetindogan, B. Ustundag, E. Turkmen, M. Wietstruck, M. Kaynak, and Y. Gurbuz, "A D-band SPDT switch utilizing reverse-saturated SiGe HBTs for Dicke-radiometers," in *Proc. 11th German Microw. Conf. (GeMiC)*, Freiburg, Germany, Mar. 2018, pp. 47–50, doi: 10.23919/GEMIC.2018.8335025.

[24] C. D. Cheon, M.-K. Cho, S. G. Rao, A. S. Cardoso, J. D. Connor, and J. D. Cressler, "A new wideband, low insertion loss, high linearity SiGe RF switch," *IEEE Microw. Wireless Compon. Lett.*, vol. 30, no. 10, pp. 985–988, Oct. 2020, doi: 10.1109/LMWC.2020.3020317.

[25] M. Margalef-Rovira, A. A. Saadi, S. Bourdel, M. J. Barragan, E. Pistono, C. Gaquiere, and P. Ferrari, "mm-Wave through-load switch for *in-situ* vector network analyzer on a 55-nm BiCMOS technology," in *Proc. 18th IEEE Int. New Circuits Syst. Conf. (NEWCAS)*, Jun. 2020, pp. 82–85, doi: 10.1109/NEWCAS49341.2020.9159829.

[26] Y. Tawfik, A. Raju, M. Varonen, M. Najmussadat, and K. A. I. Halonen, "250 GHz SiGe SPDT resonator switch," in *Proc. 15th Eur. Microw. Integr. Circuits Conf. (EuMIC)*, 2021, pp. 289–291.

[27] T. Shivan, M. Hossain, R. Doerner, S. Schulz, T. Johansen, S. Boppel, W. Heinrich, and V. Krozer, "Highly linear 90–170 GHz SPDT switch with high isolation for fully integrated InP transceivers," in *IEEE MTT-S Int. Microw. Symp. Dig.*, Boston, MA, USA, Jun. 2019, pp. 1011–1014, doi: 10.1109/MWSYM.2019.8700974.

[28] T. Shivan, M. Hossain, D. Stoppel, N. Weimann, S. Boppel, R. Doerner, W. Heinrich, and V. Krozer, "220–325 GHz high-isolation SPDT switch in InP DHBT technology," *Electron. Lett.*, vol. 54, no. 21, pp. 1222–1224, Oct. 2018, doi: 10.1049/el.2018.6028.

[29] T. Shivan, M. Hossain, R. Doerner, T. Johansen, K. Nosaeva, H. Yacoub, W. Heinrich, and V. Krozer, "A high-isolation and highly linear super-wideband SPDT switch in InP DHBT technology," in *IEEE MTT-S Int. Microw. Symp. Dig.*, Aug. 2020, pp. 1125–1128, doi: 10.1109/IMS30576.2020.9223920.

[30] Y. Kim, H. Lee, and S. Jeon, "A 220–320 GHz single-pole single-throw switch," in *Proc. IEEE Int. Symp. Radio-Freq. Integr. Technol. (RFIT)*, Aug. 2016, pp. 1–3, doi: 10.1109/RFIT.2016.7578184.

[31] C. Yi, S. H. Choi, M. Urteaga, and M. Kim, "20-Gb/s ON–OFF-keying modulators using 0.25-μm InP DHBT switches at 290 GHz," *IEEE Microw. Wireless Compon. Lett.*, vol. 29, no. 5, pp. 360–362, May 2019, doi: 10.1109/LMWC.2019.2908878.

[32] A. Margomenos, A. Kurdoghlian, M. Micovic, K. Shinohara, H. Moyer, D. C. Regan, R. M. Grabar, C. McGuire, M. D. Wetzel, and D. H. Chow, "W-band GaN receiver components utilizing highly scaled, next generation GaN device technology," in *Proc. IEEE Compound Semiconductor Integr. Circuit Symp. (CSICS)*, La Jolla, CA, USA, Oct. 2014, pp. 1–4, doi: 10.1109/CSICS.2014.6978585.

[33] F. Thome, E. Ture, P. Brückner, R. Quay, and O. Ambacher, "W-band SPDT switches in planar and tri-gate 100-nm gate-length GaN-HEMT technology," in *Proc. 11th German Microw. Conf. (GeMiC)*, Freiburg, Germany, Mar. 2018, pp. 331–334, doi: 10.23919/GEMIC.2018.8335097.

[34] F. Thome, P. Brückner, R. Quay, and O. Ambacher, "Millimeter-wave single-pole double-throw switches based on a 100-nm gate-length AlGaN/GaN-HEMT technology," in *IEEE MTT-S Int. Microw. Symp. Dig.*, Boston, MA, USA, Jun. 2019, pp. 1403–1406, doi: 10.1109/MWSYM.2019.8700955.

[35] J. Kim, W. Ko, S.-H. Kim, J. Jeong, and Y. Kwon, "A high-performance 40–85 GHz MMIC SPDT switch using FET-integrated transmission line structure," *IEEE Microw. Wireless Compon. Lett.*, vol. 13, no. 12, pp. 505–507, Dec. 2003, doi: 10.1109/LMWC.2003.819962.

[36] Z.-M. Tsai, M.-C. Yeh, M.-F. Lei, H.-Y. Chang, C.-S. Lin, and H. Wang, "DC-to-135 GHz and 15-to-135 GHz SPDT traveling wave switches using FET-integrated CPW line structure," in *IEEE MTT-S Int. Microw. Symp. Dig.*, Long Beach, CA, USA, Jun. 2005, p. 4, doi: 10.1109/MWSYM.2005.1516945.

[37] Y. Kim and S. Jeon, "mm-Wave single-pole single-throw m-HEMT switch with low loss and high linearity," *Electron. Lett.*, vol. 56, no. 14, pp. 719–721, Jul. 2020, doi: 10.1049/el.2020.0969.

[38] I. Kallfass, S. Diebold, H. Massler, S. Koch, M. Seelmann-Eggebert, and A. Leuther, "Multiple-throw millimeter-wave FET switches for frequencies from 60 up to 120 GHz," in *Proc. 38th Eur. Microw. Conf.*, Amsterdam, The Netherlands, Oct. 2008, pp. 1453–1456, doi: 10.1109/EUMC.2008.4751740.

[39] F. Thome, M. Ohlrogge, A. Leuther, M. Schlechtweg, and O. Ambacher, "An investigation of millimeter wave switches based on shunt transistors including SPDT SWITCH MMICs up to 300 GHz," in *IEEE MTT-S Int. Microw. Symp. Dig.*, San Francisco, CA, USA, May 2016, pp. 1–4, doi: 10.1109/MWSYM.2016.7540422.

[40] F. Thome and O. Ambacher, "Highly isolating and broadband single-pole double-throw switches for millimeter-wave applications up to 330 GHz," *IEEE Trans. Microw. Theory Tech.*, vol. 66, no. 4, pp. 1998–2009, Apr. 2018, doi: 10.1109/TMTT.2017.2777980.

[41] F. Thome, A. Leuther, and O. Ambacher, "Low-loss millimeter-wave SPDT switch MMICs in a metamorphic HEMT technology," *IEEE Microw. Wireless Compon. Lett.*, vol. 30, no. 2, pp. 197–200, Feb. 2020, doi: 10.1109/LMWC.2019.2958209.

[42] F. Thome, M. Ohlrogge, A. Leuther, M. Schlechtweg, and O. Ambacher, "An investigation of millimeter wave switches based on shunt transistors including SPDT SWITCH MMICs up to 300 GHz," in *IEEE MTT-S Int. Microw. Symp. Dig.*, San Francisco, CA, USA, May 2016, pp. 1–4, doi: 10.1109/MWSYM.2016.7540422.

[43] H. Mizutani, N. Iwata, Y. Takayama, and K. Honjo, "38–80 GHz SPDT traveling wave switch MMIC utilizing fully distributed FET," in *Proc. Asia–Pacific Microw. Conf.*, Yokohama, Japan, 2006, pp. 3–6, doi: 10.1109/APMC.2006.4429367.

[44] T. Shimura, Y. Mimino, K. Nakamura, Y. Aoki, and S. Kuroda, "High isolation V-band SPDT switch MMIC for high power use [HEMTs application]," in *IEEE MTT-S Int. Microw. Symp. Dig.*, Phoenix, AZ, USA, May 2001, pp. 245–248, doi: 10.1109/MWSYM.2001.966880.

[45] D. Müller, G. Scherer, U. J. Lewark, H. Massler, S. Wagner, A. Tessmann, A. Leuther, T. Zwick, and I. Kallfass, "A novel unit cell for active switches in the millimeter-wave frequency range," *J. Infr., Millim., THz Waves*, vol. 39, no. 2, pp. 161–176, Feb. 2018, doi: 10.1007/s10762-017-0454-2.

[46] F. Steinhagen, H. Massler, W. H. Haydl, A. Hulsmann, and K. Kohler, "Coplanar W-band SPDT and SPTT resonated PIN diode switches," in *Proc. 29th Eur. Microw. Conf.*, Munich, Germany, Oct. 1999, pp. 53–56, doi: 10.1109/EUMA.1999.338407.

[47] C. Yao, M. Zhou, Y. Luo, J. Zhang, X. Wei, and C. Xu, "Design of 85–105 GHz wideband traveling wave PIN diode switches and attenuators with radial stubs," *Chin. J. Electron.*, vol. 26, no. 1, pp. 218–222, Jan. 2017, doi: 10.1049/cje.2016.08.033.

[48] *Analog Devices HMC-SDD112 RF Switch Datasheet*. Accessed: Jan. 1, 2022. [Online]. Available: https://www.analog.com/media/en/technical-documentation/data-sheets/hmc-sdd112.pdf

[49] *HXI HSW100x RF Switches Datasheet*. Accessed: Jan. 1, 2022. [Online]. Available: http://www.hxi.com/Datasheets/HSW-RevE.pdf

[50] P. Song, R. L. Schmid, A. C. Ulusoy, and J. D. Cressler, "A high-power, low-loss W-band SPDT switch using SiGe PIN diodes," in *Proc. IEEE Radio Freq. Integr. Circuits Symp.*, Tampa, FL, USA, Jun. 2014, pp. 195–198, doi: 10.1109/RFIC.2014.6851695.

[51] Y. Yashchyshyn, K. Derzakowski, G. Bogdan, K. Godziszewski, D. Nyzovets, C. H. Kim, and B. Park, "28 GHz switched-beam antenna based on S-PIN diodes for 5G mobile communications," *IEEE Antennas Wireless Propag. Lett.*, vol. 17, no. 2, pp. 225–228, Feb. 2018, doi: 10.1109/LAWP.2017.2781262.

[52] Y. Yashchyshyn, K. Derzakowski, P. R. Bajurko, J. Marczewski, and S. Kozłowski, "Time-modulated reconfigurable antenna based on integrated S-PIN diodes for mm-wave communication systems," *IEEE Trans. Antennas Propag.*, vol. 63, no. 9, pp. 4121–4131, Sep. 2015, doi: 10.1109/TAP.2015.2444425.

[53] A. H. Zahr, L. Y. Zhang, C. Dorion, A. Deveautour, A. Beneteau, R. Stefanini, and P. Blondy, "RF-MEMS switches for millimeter-wave applications," in *Proc. Eur. Microw. Conf. Central Eur. (EuMCE)*, Prague, Czech Republic, 2019, pp. 336–338.

[54] S. Reyaz, C. Samuelsson, R. Malmqvist, M. Kaynak, and A. Rydberg, "Millimeter-wave RF-MEMS SPDT switch networks in a SiGe BiCMOS process technology," in *Proc. 7th Eur. Microw. Integr. Circuit Conf.*, Amsterdam, The Netherlands, Oct. 2012, pp. 691–694.

[55] M. Ulm, J. Schobel, M. Reimann, T. Buck, J. Dechow, R. Müller-Fiedler, H.-P. Trah, and E. Kasper, "Millimeter-wave microelectromechanical (MEMS) switches for automotive surround sensing systems," in *Top. Meeting Silicon Monolithic Integr. Circuits RF Syst., Dig. Papers*, Grainau, Germany, 2003, pp. 142–149, doi: 10.1109/SMIC.2003.1196691.

[56] S. T. Wipf, A. Göritz, M. Wietstruck, C. Wipf, B. Tillack, and M. Kaynak, "D–band RF–MEMS SPDT switch in a 0.13 μm SiGe BiCMOS technology," *IEEE Microw. Wireless Compon. Lett.*, vol. 26, no. 12, pp. 1002–1004, Dec. 2016, doi: 10.1109/LMWC.2016.2623245.

[57] S. T. Wipf, A. Goritz, C. Wipf, M. Wietstruck, A. Burak, E. Turkmen, Y. Gurbuz, and M. Kaynak, "240 GHz RF-MEMS switch in a 0.13 μm SiGe BiCMOS technology," in *Proc. IEEE Bipolar/BiCMOS Circuits Technol. Meeting (BCTM)*, Oct. 2017, pp. 54–57, doi: 10.1109/BCTM.2017.8112910.

[58] Z. Baghchehsaraei, U. Shah, S. Dudorov, G. Stemme, J. Oberhammer, and J. Åberg, "MEMS 30 μm-thick W-band waveguide switch," in *Proc. 42nd Eur. Microw. Conf.*, Amsterdam, The Netherlands, Oct. 2012, pp. 1055–1058, doi: 10.23919/EuMC.2012.6459114.

[59] Z. Baghchehsaraei, U. Shah, J. Åberg, G. Stemme, and J. Oberhammer, "Millimeter-wave SPST waveguide switch based on reconfigurable MEMS surface," in *IEEE MTT-S Int. Microw. Symp. Dig.*, Seattle, WA, USA, Jun. 2013, pp. 1–4, doi: 10.1109/MWSYM.2013.6697774.

[60] S. Shekhar, K. J. Vinoy, and G. K. Ananthasuresh, "Low-voltage high-reliability MEMS switch for millimeter wave 5G applications," *J. Micromech. Microeng.*, vol. 28, no. 7, Jul. 2018, Art. no. 075012.

[61] P. Sharma, J. Perruisseau-Carrier, C. Moldovan, and A. M. Ionescu, "Electromagnetic performance of RF NEMS graphene capacitive switches," *IEEE Trans. Nanotechnol.*, vol. 13, no. 1, pp. 70–79, Jan. 2014, doi: 10.1109/TNANO.2013.2290945.

[62] P. Borodulin, N. El-Hinnawy, C. R. Padilla, A. Ezis, M. R. King, D. R. Johnson, D. T. Nichols, and R. M. Young, "Recent advances in fabrication and characterization of GeTe-based phase-change RF switches and MMICs," in *IEEE MTT-S Int. Microw. Symp. Dig.*, Honolulu, HI, USA, Jun. 2017, pp. 285–288, doi: 10.1109/MWSYM.2017.8059098.

[63] T. Singh and R. R. Mansour, "Monolithic PCM based miniaturized T-type RF switch for millimeter wave redundancy switch matrix applications," in *IEEE MTT-S Int. Microw. Symp. Dig.*, Boston, MA, USA, Jun. 2019, pp. 658–660, doi: 10.1109/MWSYM.2019.8700946.

[64] T. Singh and R. R. Mansour, "Experimental investigation of performance, reliability, and cycle endurance of nonvolatile DC–67 GHz phase-change RF switches," *IEEE Trans. Microw. Theory Techn.*, vol. 69, no. 11, pp. 4697–4710, Nov. 2021, doi: 10.1109/TMTT.2021.3105413.

[65] T. Singh and R. R. Mansour, "Scalable mmWave non-volatile phase change GeTe-based compact monolithically integrated wideband digital switched attenuator," *IEEE Trans. Electron Devices*, vol. 68, no. 5, pp. 2306–2312, May 2021, doi: 10.1109/TED.2021.3069729.

[66] C. Hillman, P. A. Stupar, J. B. Hacker, Z. Griffith, M. Field, and M. Rodwell, "An ultra-low loss millimeter-wave solid state switch technology based on the metal–insulator–transition of vanadium dioxide," in *IEEE MTT-S Int. Microw. Symp. Dig.*, Tampa, FL, USA, Jun. 2014, pp. 1–4, doi: 10.1109/MWSYM.2014.6848479.

[67] C. Hillman, P. Stupar, and Z. Griffith, "Scaleable vanadium dioxide switches with submillimeterwave bandwidth: VO_2 switches with impoved RF bandwidth and power handling," in *Proc. IEEE Compound Semiconductor Integr. Circuit Symp. (CSICS)*, Miami, FL, USA, Oct. 2017, pp. 1–4, doi: 10.1109/CSICS.2017.8240450.

[68] N. El-Hinnawy, P. Borodulin, A. Ezis, C. Furrow, C. Padilla, M. King, E. Jones, B. Wagner, J. Paramesh, J. Bain, D. Nichols, and R. M. Young, "Substrate agnostic monolithic integration of the inline phase-change switch technology," in *IEEE MTT-S Int. Microw. Symp. Dig.*, San Francisco, CA, USA, May 2016, pp. 1–4, doi: 10.1109/MWSYM.2016.7540103.

[69] M. Kim, S. Park, A. Sanne, S. K. Banerjee, and D. Akinwande, "Towards mm-wave nanoelectronics and RF switches using MoS_2 2D semiconductor," in *IEEE MTT-S Int. Microw. Symp. Dig.*, Philadelphia, PA, USA, Jun. 2018, pp. 352–354, doi: 10.1109/MWSYM.2018.8439336.

[70] F. Yang, X. Wu, X. Guo, and Y. Xu, "A design of SPDT switch using graphene device," in *Proc. IEEE Int. Symp. Antennas Propag. USNC/URSI Nat. Radio Sci. Meeting*, Vancouver, BC, Canada, Jul. 2015, pp. 1658–1659, doi: 10.1109/APS.2015.7305218.

[71] K. Pan, T. Leng, X. Zhang, and Z. Hu, "Design and modeling of back gated graphene based RF switch with CPW transmission line on a high resistivity silicon substrate," in *Proc. 10th UK-Eur.-China Workshop Millim. Waves THz Technol. (UCMMT)*, Liverpool, U.K., Sep. 2017, pp. 1–2, doi: 10.1109/UCMMT.2017.8068505.

[72] P. C. Theofanopoulos and G. C. Trichopoulos, "Modeling of submillimeter wave coplanar waveguide graphene switches," in *Proc. IEEE Int. Symp. Antennas Propag. USNC-URSI Radio Sci. Meeting*, Atlanta, GA, USA, Jul. 2019, pp. 1527–1528, doi: 10.1109/APUSNCURSINRSM.2019.8889029.

[73] B. Wu, Y. Zhang, H. Zu, C. Fan, and W. Lu, "Tunable grounded coplanar waveguide attenuator based on graphene nanoplates," *IEEE Microw. Wireless Compon. Lett.*, vol. 29, no. 5, pp. 330–332, May 2019, doi: 10.1109/LMWC.2019.2908034.

[74] A.-Q. Zhang, Z.-G. Liu, L. Wei-Bing, and H. Chen, "Graphene-based dynamically tunable attenuator on a coplanar waveguide or a slotline," *IEEE Trans. Microw. Theory Techn.*, vol. 67, no. 1, pp. 70–77, Jan. 2019, doi: 10.1109/TMTT.2018.2875078.

[75] P. Sharma, J. Perruisseau Carrier, and A. M. Ionescu, "Nanoelectromechanical microwave switch based on graphene," in *Proc. 14th Int. Conf. Ultimate Integr. Silicon (ULIS)*, Coventry, U.K., Mar. 2013, pp. 189–192, doi: 10.1109/ULIS.2013.6523516.

[76] Y. Litun, V. Litun, O. Kononenko, M. Chichkov, and D. Borisenko, "Technological features of graphene-based RF NEMS capacitive switches on a semi-insulating substrate," in *Proc. Photon. Electromagn. Res. Symp. Spring (PIERS-Spring)*, Rome, Italy, 2019, pp. 3666–3672, doi: 10.1109/PIERS-Spring46901.2019.9017225.

[77] Y. Yashchyshyn, P. Bajurko, J. Sobolewski, P. Sai, A. Przewłoka, A. Krajewska, P. Prystawko, M. Dub, W. Knap, S. Rumyantsev, and G. Cywiński, "Graphene/AlGaN/GaN RF switch," *Micromachines*, vol. 12, no. 11, p. 1343, Oct. 2021, doi: 10.3390/mi12111343.

[78] J. Liu, Z. U. Khan, C. Wang, H. Zhang, and S. Sarjoghian, "Review of graphene modulators from the low to the high figure of merits," *J. Phys. D, Appl. Phys.*, vol. 53, no. 23, Jun. 2020, Art. no. 233002, doi: 10.1088/1361-6463/ab7cf6.

[79] P. Weis, J. L. Garcia-Pomar, M. Höh, B. Reinhard, A. Brodyanski, and M. Rahm, "Spectrally wide-band terahertz wave modulator based on optically tuned graphene," *ACS Nano*, vol. 6, no. 10, pp. 9118–9124, Oct. 2012, doi: 10.1021/nn303392s.

[80] Q.-Y. Wen, W. Tian, Q. Mao, Z. Chen, W.-W. Liu, Q.-H. Yang, M. Sanderson, and H.-W. Zhang, "Graphene based all-optical spatial terahertz modulator," *Sci. Rep.*, vol. 4, no. 1, p. 7409, May 2015, doi: 10.1038/srep07409.
[81] *Gotmic gSSS0015 SPST Switch Datasheet*. Accessed: Jan. 1, 2022. [Online]. Available: https://www.gotmic.se/documents/gSSS0015_Rev_A01-17.pdf
[82] *Keysight TC950 SPDT MMIC Switch Datasheet*. Accessed: Jan. 1, 2022. [Online]. Available: https://www.keysight.com/zz/en/assets/7018-07156/data-sheets/5991-4766.pdf

JAKUB SOBOLEWSKI (Graduate Student Member, IEEE) received the B.S. degree in electronics engineering from the Bialystok University of Technology, Bialystok, Poland, in 2014, and the M.S. degree in telecommunications from the Warsaw University of Technology, Warsaw, Poland, in 2017, where he is currently pursuing the Ph.D. degree in telecommunications. His research interests include the microwave and millimeter wave antenna design, microwave material characterization, millimeter wave integrated circuits, and integration of high frequency devices.

YEVHEN YASHCHYSHYN (Senior Member, IEEE) received the M.E. degree from Lviv Polytechnic National University, Lviv, Ukraine, in 1979, the Ph.D. degree from the Moscow Institute of Electronics and Mathematics, Moscow, Russia, in 1986, and the D.Sc. (Habilitation) degree from the Warsaw University of Technology (WUT), Warsaw, Poland, in 2006. In 2016, he was promoted to a Professor. Since 1999, he has been with the Institute of Radioelectronics and Multimedia Technology, WUT, where he is currently a Professor and the Head of the Sub-Terahertz Technology Division. He has authored more than 250 technical articles and has authored or coauthored five books. He holds several patents. His current research interests include antenna theory and techniques, smart beamforming, reconfigurable antennas, radio-over-fiber techniques, and materials characterization, including ferroelectric ceramic-polymers composites investigation up to subterahertz frequency.